ISBN: 978-3-95450-192-2 doi:10.18429/JACoW-IBIC2017-TU2AB1

INTEGRATED PHOTONICS TO THE RESCUE OF FEMTOSECOND BEAM DIAGNOSTICS

Franz X. Kärtner
Center for Free-Electron Laser Science, Deutsches Elektronen-Synchrotron and
Universität Hamburg, Germany
also at Research Laboratory of Electronics, Massachusetts Institute of Technology, Cambridge, USA

Abstract

Beam instrumentation has always been using results from neighbouring communities. Over the last 10 years, a number of beam instruments and systems have successfully adopted optical solutions, pushing performances from ps to fs, exploiting optical set-ups or photonic components. A major advance for beam diagnostics and instrumentation was the introduction of an optical pulsed timing distribution system using low jitter mode-locked lasers. An outlook on future advances using integrated optical components will be given. The ultra low jitter optical pulse trains already present in today's facilities may also lend themselves to advanced photonic analogto-digtial convertors. Progress towards such devices especially in a practical integrated format and first demonstrations are discussed.

INTRODUCTION

Modern photon science facilities, such as X-ray Free-Electron Lasers (XFEL) are becoming more and more combined accelerator and laser facilities. Lasers play an essential role starting from the photo injector laser creating the electron bunch in the gun, over a potential seed laser down to the experimental station, which usually houses a pump and/or probe lasers to excite the sample under investigation or probe it at optical frequencies. Over the last decade great progress has been made in synchronizing all lasers as well as critical microwave sources in such facilities within 10 fs rms using optical techniques. This is at least one order of magnitude better than possible with microwave techniques. In this tutorial, we first review the principles behind the optical synchronization techniques and show their further development to the sub-femtosecond level. Then we give an outlook how the low jitter properties of mode-locked lasers can be further harnessed to advance beam diagnostics at the example of photonic analog-to-digital conversion (ADC), which becomes only useful in an integrated optical package. This is made possible by exploiting the low jitter properties of mode-locked lasers. More precisely photonically assisted ADC, where optics is only used to eliminate aperture jitter and enable demultiplexing to lower rate channels, which then can be electronically digitized with the required number of bits may potentially enable a thousand fold enhancement in the resolution-sampling rate product when compared to current electronic ADCs.

JITTER OF MODE-LOCKED LASERS

The noise properties of mode-locked lasers were theoretically studied in the framework of soliton perturbation theory by Haus and Mecozzi in their seminal paper published in 1993 [1]. It successfully predicted the noise behavior of many mode-locked solid-state and fiber lasers [2–5]. Recently, it was discussed that the scaling of phase diffusion found in the Haus/Mecozzi model is generally applicable, independent from soliton effects [6]. Here, we present a simple intuitive picture of the timing jitter scaling when transitioning from the traditional case of a microwave oscillator generating a microwave signal at let's say 10 GHz to the case of a mode-locked laser generating an optical pulse train with 100-fs pulses [7].

Figure 1 shows the time-domain picture of microwave signals and optical pulse trains when emitted from an ensemble of microwave oscillators and mode-locked lasers, respectively. The zero crossings of the microwave signal and the pulse positions of the optical pulse train undergo a random walk due to the fundamental noise sources in the signal generation processes such as output coupling and compensation of cavity losses by gain. For the microwave oscillator, this fundamental noise is additive noise due to the losses of the passive cavity (internal as well as output coupling losses) and the reservoirs in the amplifying medium. Clearly, the noise contributions of gain and loss are uncorrelated. The noise energy added to the cavity field within a cavity decay time due to the losses is determined by the fluctuation-dissipation theorem, and it must be equal to kT in thermal equilibrium.

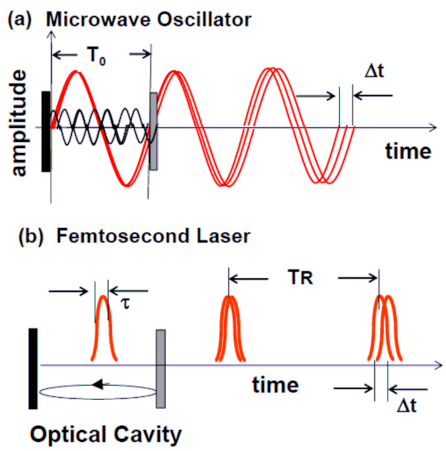

Figure 1: Random walk of (a) the phase in a microwave oscillator and (b) the pulse position in a mode-locked laser due to noise sources in the generation process [7]

ISBN: 978-3-95450-192-2 doi:10.18429/JACoW-IBIC2017-TU2AB1

For the case of a lossy optical resonator, the equivalent noise energy added during a cavity decay time is $\hbar\omega_c$ instead of kT to be conform with quantum mechanics. Therefore, one can show that the diffusion rates for timing of a microwave oscillator and mode-locked laser follows Eq. (1) and (2).

$$\frac{d}{dt} < \Delta t_{\mathrm{RF}}^2 > \sim T_0^2 \cdot \frac{1}{W_{\mathrm{mode}}} \cdot \frac{kT}{\tau_{cav}}, \quad (1)$$

$$\frac{d}{dt} < \Delta t_{\mathrm{ML}}^2 > \sim \tau^2 \cdot \frac{1}{W_{\mathrm{pulse}}} \cdot \frac{\hbar\omega_c}{\tau_{cav}}. \quad (2)$$

The corresponding diffusion rates are inversely proportional to the energy stored in the resonator and scale proportional to the characteristic timescale of the pulse or signal, which is the period in the case of the microwave oscillator and the pulse width in the case of a short pulse laser. This is obvious by inspection, if a small random signal is added to one of the waveforms shown in Fig. 1. The uncertainty in the zero-crossing of the signals is less with increasing slope of the signal, which is directly proportional to its bandwidth. It is the short pulse duration of femtosecond lasers, typically 100 fs, that makes the scaling of timing jitter for femtosecond lasers so much better than timing jitter in microwave oscillators of typically 10 GHz frequency with 100 ps period. The factor of 1000 does not materialize completely due to the higher noise of optical amplifiers versus microwave amplifiers, versus kT, of roughly 40, at room temperature. Still this makes short pulse lasers superb optical clocks, and their pulse trains can be easily and robustly distributed over large distances with very low loss via optical fibers.

HIGH RESOLUTION TIMING JITTER CHARACTERIZATION

A challenge arising in the pursuit of low timing jitter sources is the actual characterization of the timing jitter once approaching the 10 fs level, which is about the level that is supported by commerical signal source analyzers. For phase noise characterization of microwave oscillators, two techniques, the phase detector method and the phase delay method are usually used [8].

The phase detector method is limited by the noise of the reference oscillator used in the measurement process, which is on the 10 fs range for offset frequencies greater than 10 kHz for current microwave synthesizers implemented in signal source analyzers. The phase delay method is limited to the high frequency range because of the limited microwave delays that can be implemented with reasonable loss. The timing jitter of mode-locked lasers can be determined by photodetecton of the pulse train, followed by subsequent filtering of one of the harmonics of the resulting microwave signal and using the microwave techniques discussed. However, the limitations discussed above apply, and in addition, amplitude-to-phase noise conversion [9] in the photodetection process may further degrade the quality of the measurement. Since we have optical sources that are superior to their microwave counterparts in terms of timing jitter, it is therefore necessary to develop techniques that make use of optics to characterize the timing jitter with higher resolution than is possible in the microwave domain. This is possible by using balanced optical cross correlation (BOC) [10, 11]. An implemenation, that is especially advantageous in the 1.55 µm band, is shown in Fig. 2(a).

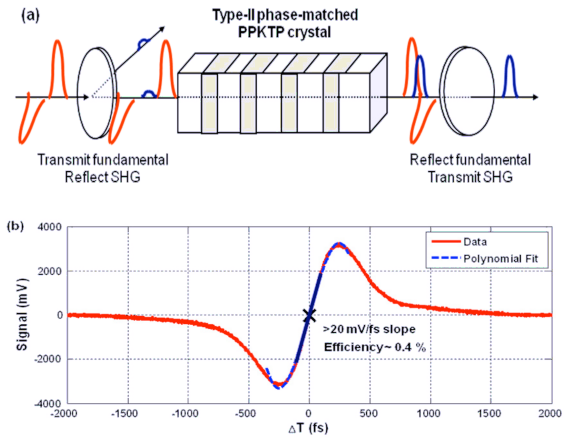

Figure 2: (a) Balanced optical cross correlator (BOC) based on PPKTP [11] and (b) measured cross correlation signal as a function of delay between input pulses [7].

A type-II phase-matched periodically poled KTP-crystal (PPKTP) [12] is used to generate a balanced cross correlation signal of two pulses with orthogonal polarization entering from the left. Due to the birefringence of the crystal (typically a few mm long) 100 fs pulses walk through each other by about 500 fs. Depending on their relative position at the entrance point into the crystal, a certain amount of second harmonic light (SHG) is generated in the forward direction and coupled out via a dichroic mirror. The remaining infrared pulses are reflected back into the crystal and continue to walk through each other generating another amount of SHG, which is then separated with a dichroic beamsplitter from the infrared light leaving the crystal. Each SHG component generated during the forward and backward propagation is then directed to the input of a balanced detector, which generates the cross correlation signal depicted in Fig. 2(b). Even for moderate pulse energies of a few tenths of pJ, a signal with a slope of 20 mV per femtosecond of delay between the two input pulses is derived. In comparison, typical microwave mixers generate timing error signals on the order of mVs per femtosecond delay for 10 GHz microwave signals. Therefore, such a balanced cross correlator can resolve on the order of 10 attoseconds of timing jitter. This device can essentially replace the microwave mixer in the established phase detector and phase delay method and translate them into a timing detector and timing delay method [8], see Fig. 3(a) for timing detector method used in the following. Figure 3(b) shows the timing jitter spectral density of the low jitter laser Origami from the company OneFive measured with the timing detector method above 1 kHz. The integrated timing jitter of the laser for offset frequencies above 1 kHz is less than 0.25 fs [13]. Such low jitter lasers,

ISBN: 978-3-95450-192-2 doi:10.18429/JACoW-IBIC2017-TU2AB1

when disciplined in repetiton rate to a microwave reference for long term stability, can be used as an optical master oscillator (OMO) in femtosecond to attosecond precision timing distribution systems.

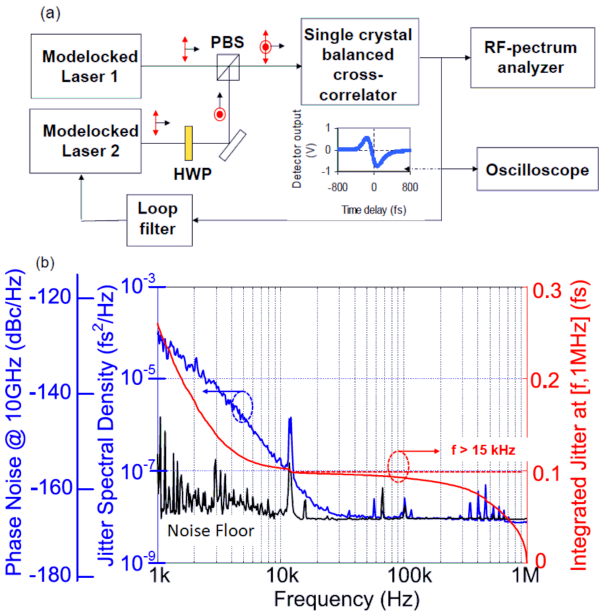

Figure 3: (a) Timing jitter measurement of a mode-locked laser using two identical lasers and an optical cross correlator based on PPKTP using the timing detector method [6] and (b) Timing jitter spectral density measurement of a low jitter laser (OneFive - Origami) using the timing detector method above 1 kHz.

OPTICAL PULSED TIMING DISTRIBUTION SYSTEM

A conceptual layout for a timing distribution system (TDS) for a large scale facility such as an X-ray FreeElectron Laser (XFEL) using the low jitter properties of mode-locked lasers is sketched in Fig. 4.

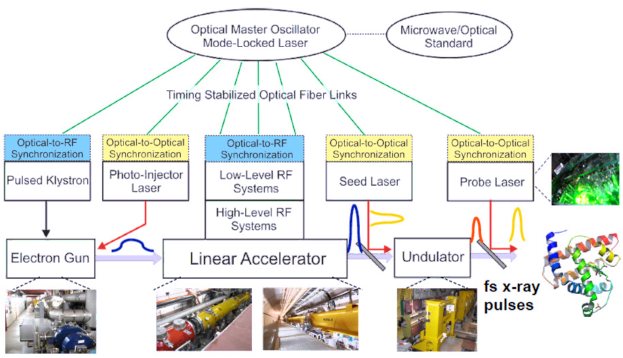

Figure 4: Schematic layout of an optical pulsed timing distribution system for a seeded XFEL facility.

The low jitter pulse train from a repetition rate stabilized OMO is distributed over timing stabilized fiber links to all timing critical positions within the facility. At the fiber link ends additional BOCs can synchronize lasers at the same wavelength (1.5 mm) as the OMO to the output pulse stream with sub-femtosecond precision or two-color balanced cross correlators can be implemented (TC-BOC) to tightly lock any other low jitter lasers to the precision fiber network [14].

Timing Stabilized Fiber Link

At the core of a TDS are timing stabilized fiber links, that use a BOC for precision measurement of the time of flight of femtosecond laser pulses through the fiber link (Fig. 5). Assuming that forward and backward propagation times are identical, the slow and fast expansion of the fiber can be sensed with attosecond precision and a PZT-based fiber stretcher, and, if necessary additional mechanical delays, can compensate for it to keep the time of flight within a round-trip fixed. A necessity is to use a dispersion compentated fiber link, by combining for example standard single-mode fiber (SMF) with standard dispersion shifted fiber (DCF). Limitations may be due to polarization mode dispersion (PMD) that may break the symmetry between the forward and backward propagating path and makes the link also sensitive to perturbations.

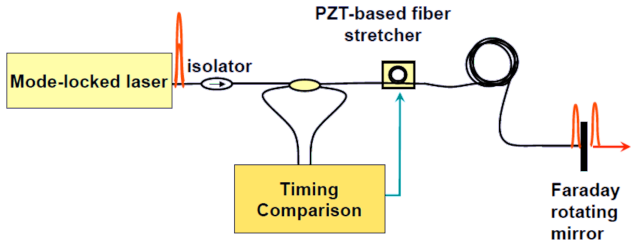

Figure 5: Schematic layout of a timing stabilized fiber link.

For that reason PM-fiber links have been developed recently [15]. For example, Fig. 6 shows the out-of-loop measured drifts between two fiber links in a commercal 16-link TDS over 60 hours, where some links are exposed to plus/minus 1°C temperature fluctuations using PMdispersion compensated links. Clearly, the rms drifts between links stays well below 1 fs.

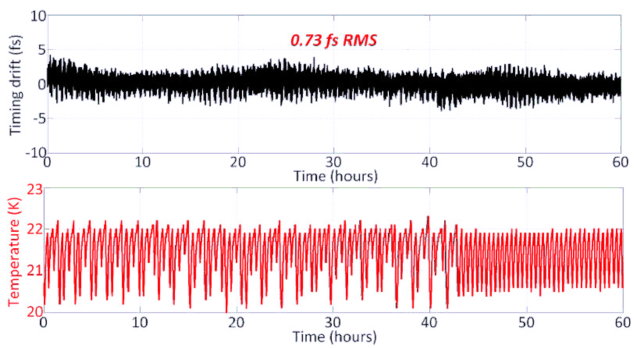

Figure 6: Out-of-loop measurment of timing drift between two fiber links in a commercal 16-link TDS over 60 hours, where some links are exposed to plus/minus 1° C temperature fluctuations [16].

ISBN: 978-3-95450-192-2 doi:10.18429/JACoW-IBIC2017-TU2AB1

Balanced Optical Microwave Phase Detector

Synchronization of microwave signals with optical pulse trains can be implemented using photo-detection filtering and implementation of a classic phase locked loop (PLL). However, nonideal behavior of the photo- de detection process such as AM-to-PM conversion and temperature pendent phase shifts in detectors and mixers typically limits timing drifts in such PLLs to about 100 fs. Careful selection of photo-receivers and temperature stabilization may help to get to the 10-fs range. To overcome these problems, a differentially-biased Sagnac fiber-loop and synchronous detection is used to implement a balanced optical-microwave phase detector (BOM-PD) [17]. Figure 7 shows the schematic a BOMPD. An optical pulse train with a repetition rate of fR is sent to the Sagnac fiber-loop. A reference signal with a frequency (n+1/2)fR is generated from the input pulse train for biasing of the Sagnac loop in a differential way and for synchronous detection. Both the microwave signal from the VCO and the reference signal are applied to the modulator. For high-frequency VCO signals (NfR), the traveling-wave nature of the phase modulator ensures a differential phase shift between the counter propagating pulses. The resulting output pulse train from the Sagnac loop is intensity-modulated at half the repetition rate, fR/2, as shown in Fig. 7. The modulation depth is, to first order, proportional to the phase error between the pulse train and the microwave signal from the VCO. A detailed quantitative derivation of this relationship can be found in [18]. The amplitude modulation is down converted into a baseband signal to drive the VCO.

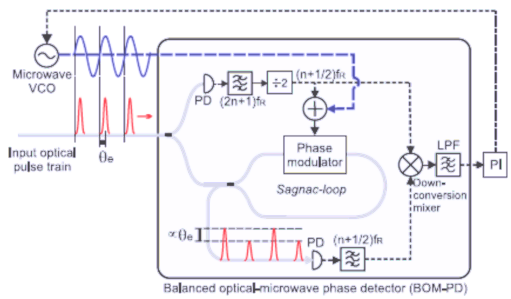

Figure 7: Schematic of the microwave signal to optical pulse train synchronization using a BOM-PD. The phase error is converted to an intensity modulation at the output of the differentially biased Sagnac loop. By synchronous detection using the downconversion mixer, a baseband error signal is generated from the BOM-PD [18].

When the PLL is locked, the pulse train is aligned with the zero crossings of the microwave signal. To demonstrate the quality of optical-to-microwave synchronization using the BOM-PD, we used two BOM-PDs: one for synchronizing the microwave signal with the optical pulse train, and the other for monitoring the out-of-loop timing jitter over 10 hours (more detailed information on the experiment and measurement setup can be found in [19]).

Figure 8 summarizes the measurement results. The top figure shows the out-of-loop SSB phase noise density at 10.225 GHz and the corresponding integrated timing jitter between the microwave signal and the optical pulse train. The bottom figure shows the out-of-loop drift, which is also slightly below 1 fs measured over 10 hours.

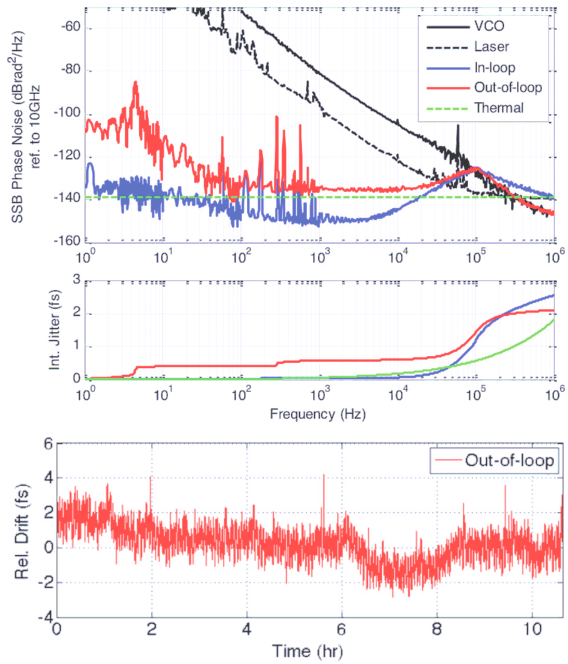

Figure 8: Out-of-loop measurement of timing jitter and drift of an optical-PLL between a 200 MHz laser (Menlo Systems M-Comb) and at 10.225 GHz VCO using a BOM-PD as the phase detector; (top) Short-term timing jitter measurements: single sideband residual phase error spectra; (bottom) integrated RMS timing jitter from 1 Hz; 1 fs conservative estimate for BOMPD residual noise floor up to 100-kHz; (bottom) The rms drift is also below 1 fs and peak-to-peak drift is less than 7 fs over 10 hours [19].

Attosecond Laser-Microwave Networks

Numerous improvements have been made over the years to push the precision of both BOCs and BOMPDs well below the 1-fs level and to minimize the interplay of nonlinear pulse propagation and laser noise in the fiber link. This results in km-scale networks of lasers and microwave sources synchronized to the sub-femtosecond level, see Fig. 9 [20].

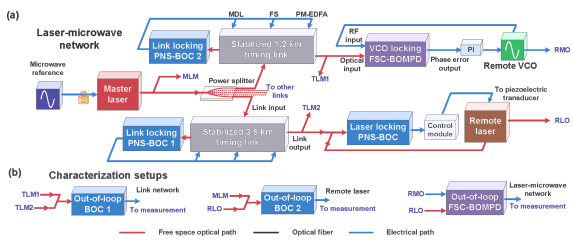

Figure 9: (a) Laser-microwave network (VCO, voltage-controlled oscillator); (b) Out-of-loop setups [20].

Figure 10 shows the integrated jitter and drift of the sub-circuits as well as the overall laser-microwave network not exceeding in total the 1 fs barrier over 10 hours.

ISBN: 978-3-95450-192-2 doi:10.18429/JACoW-IBIC2017-TU2AB1

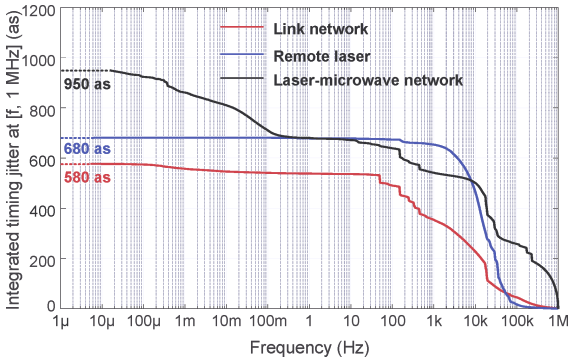

Figure 10: Integrated timing jitter of three characterization setups in the laser-microwave network [20].

Integrated Balanced Optical Cross Correlators

Further advances in pulsed optical timing distribution can be expected for implementation, robustness, size, cost as well as precision by introducing integrated optical components. At this point a waveguide BOC was fabricated using ion-exchanged waveguides in potassium titanyl phosphate (KTP), which was chosen because of its nonlinear optical properties, high-power handling, and wide acceptance bandwidth [21]. The sensitivity of the BOC device was measured using a 1560 nm mode-locked femtosecond laser with a pulse duration of 200 fs and 10 mW of total input power. The laser pulse was split into two paths with the polarization of one path rotated by 90 degrees. By varying the arrival time of the pulses, the balanced cross correlation trace of the device is generated (Fig. 11). The measured sensitivity is 79 mV/fs, a factor of 8 improvement over a previous free-space coupled bulk device.

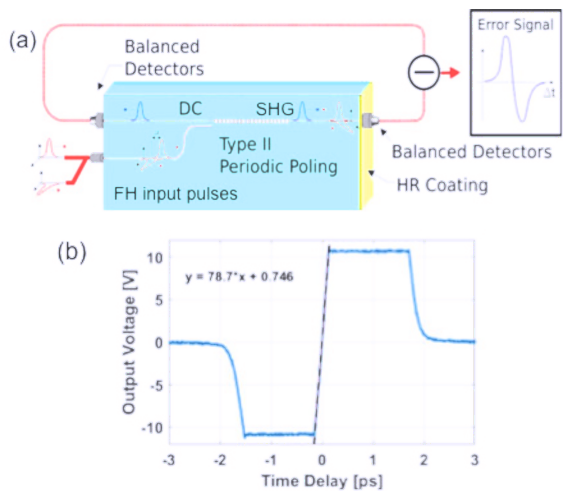

Figure 11: (a) Integrated waveguide BOC; (b) Measured balanced cross correlation of the integrated BOC device. The slope of the line is the sensitivity (79 mV/fs) [22].

PHOTONIC ADC

The field of electronic data conversion has witnessed significant progress over the last decade. With the unity gain frequency of CMOS technology reaching hundreds of gigahertz and matured SiGe technology, data converters based on the silicon platform operating at sampling rates of tens of GSa/s now exist. For instance, Fujitsu Inc. recently introduced a 65 GSa/s ADC in CMOS [23]. Prior to that, Nortel Inc. had demonstrated a 40 GSa/s CMOS ADC [24], and Rensselaer Polytechnic Institute had introduced its 40 GSa/s SiGe ADC [25]. While radio frequency (RF) electronic data converters are now running at unprecedented sampling rates, their performance, as defined by effective number of bits (ENOB), has not improved commensurately. A major factor limiting the progress towards higher rates and resolutions is aperture jitter, i.e. inability of ADCs to sample at precisely defined times. Figure 12 shows ENOB as a function of input frequency for high-performance electronic ADCs, as reviewed by Walden [26], including some ADCs that have appeared afterwards. Dashed lines represent ENOB limits due to jitter.

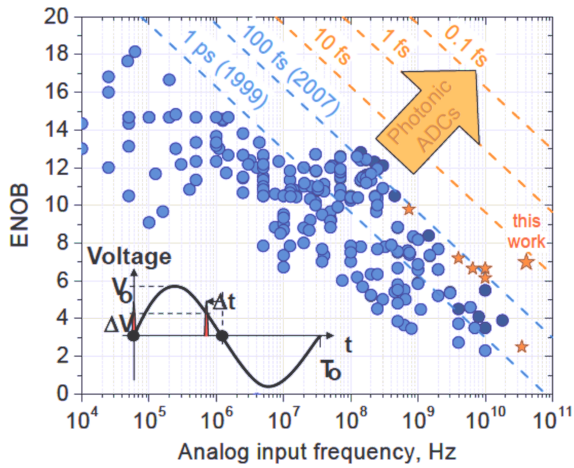

Figure 12: "Walden plot" showing ENOB of existing ADCs as a function of analog input frequency. Each point represents an ADC: blue circles correspond to the ADCs from Walden's survey of ADCs as of late 2007 [26], and dark blue circles correspond to some high-performance ADCs that have been demonstrated since 2007. The dashed lines are locii of constant values of aperture jitter, as indicated next to the lines together with the year when this jitter value was achieved. Photonic ADCs, operating with very low timing jitter, are envisaged to bring ADC performance to new levels, as indicated by the arrow labeled "Photonic ADCs". Some high-performance wideband photonic ADC results are shown with orange stars, with the large star corresponding to the result we discuss here in some detail. Details on data points used in this plot can be found in [26]. The figure is taken from [27].

The best electronic ADCs deliver jitter levels of 60-80 fs in the 100-400 MHz frequency range; reducing the jitter further becomes increasingly difficult, especially beyond gigahertz frequencies, and if the past is a good prediction for the future, it will take nearly a decade to improve the jitter performance by an order of magnitude [26]. As discussed

ISBN: 978-3-95450-192-2 doi:10.18429/JACoW-IBIC2017-TU2AB1

above, ultra-stable mode-locked laser sources with jitter levels many orders of magnitude lower exist today; if used for sampling, they could improve ADC performance by orders of magnitude.

The potential of the photonic approach is demonstrated by sampling a 41 GHz signal with record 7.0 ENOB with a discrete-component photonic ADC [28]. This performance is equivalent to 15 fs jitter, a significant improvement over today's state-of-the-art. A practical photonic ADC must be integrated on a chip, which can be realized using rapidly developing silicon photonics technology There are two standard architectures for photonic ADC systems. The first, known as photonic time stretch, utilizes dispersion of a chirped optical pulse to temporally magnify a segment of a wideband signal to be sampled [29]. After magnification, the signal can be electronically sampled and quantized at a lower sample rate. Photonic time stretch systems suffer due to dispersion-induced attenuation of high-frequency components in the analog waveform. A second photonic ADC architecture is known as time-interleaved optical sampling. With this approach, a stream of pulses or a single chirped pulse is used to sample the analog signal at a high sample rate. After sampling, the pulses are separated into several lower-rate streams using time-division multiplexing (TDM) [30] or wavelength-division multiplexing (WDM) [31] techniques. The TDM approach simplifies the requirements on the optical sampling source. However, the TDM demultiplexer can be difficult to implement and may limit the maximum sample rate. With the WDM approach the multiwavelength stream of optical pulses is de-interleaved using passive WDM demultiplexers, see Fig. 13.

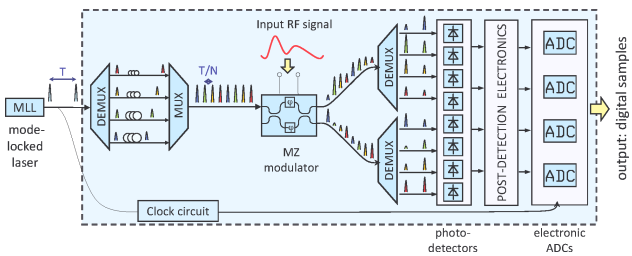

Figure 13: Layout of the photonic ADC studied in this work. The components of the ADC inside the dashed box can ultimately be integrated on a single electronic-photonic chip using a silicon photonics approach [27].

A low-jitter femtosecond laser, as described above, with repetition rates of a few hundred MHz or a few GHz emits a stream of pulses that is dispersed. Dispersion is chosen such that the chirped pulses cover the time interval between the pulses. The RF-waveform to be sampled is imprinted on the chirped pulse stream via an electro-optic modulator. The optical output is channelized via a WDMfilter bank with precisely-tuned center frequencies that map to certain sampling times. The signal from each channel, which corresponds to time interleaved sample sequence, can be separately digitized in low-rate highresolution ADCs, which are fed by an on-chip Si/Ge photodetector array converting each channel at a much lower rate into electrical signals. The total sampling rate is then the optical clock rate, i.e., the repetiton rate of the modelocked laser, times the number of WDM channels.

Figure 14 (a) shows only one of the integrated optical components necessary towards such an integrated ADC, the two matched 20-channel filter banks fabricated on a silicon chip. Each bank is intended to demultiplex one of the two complementary outputs of the MZ modulator. The filters are second-order microring-resonator filters. Microheaters fabricated on top of each ring are used to thermally tune resonant frequencies in order to compensate for fabrication errors and put the resonances on a desired grid. Figure 14(b) shows the measured transmission characteristics of the 20 channels; the overlapping red and the blue lines correspond to the two matched banks.

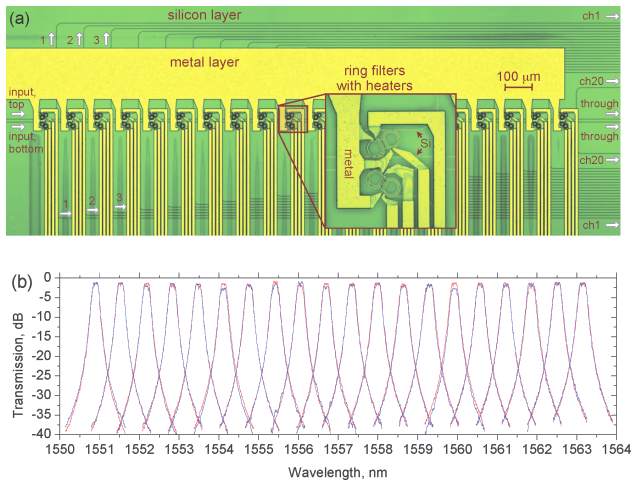

Figure 14: (a) Photograph of two matched 20-channel filter banks fabricated on a silicon chip. (b) Measured transmission of the 20 channels; the overlapping red and the blue lines correspond to the two matched banks [27].

CONCLUSION

The low jitter of femtosecond lasers, reaching attosecond levels in the high frequency range, enables much progress in beam diagnostic, controls and synchronization in accelerator and light source facilities. This development has by far not reached its ends. Advances in integrated optics, in combination with femtosecond lasers, either on or off chip or using the output from fiber distribution systems, enables photonic ADCs with much increased bandwidth-resolution products. Several orders of magnitude in improvement are possible.

ACKNOWLEDGEMENT

The author is indebted to students, postdocs and collaborators at both MIT and DESY, who worked over the last 15 years on the topics presented in this paper. Support through AFOSR, DOE, DARPA and the Helmholtz Association that supported various aspects of this work is gratefully acknowledged.

ISBN: 978-3-95450-192-2 doi:10.18429/JACoW-IBIC2017-TU2AB1

REFERENCES

[1] H. A. Haus and A. Mecozzi, "Noise of mode-locked lasers," *IEEE J. Quantum Electron.*, vol. 29, pp. 983, March 1993.

[2] M. E. Grein, L. A. Jiang, H. A. Haus, E. P. Ippen, C. McNeilage, J. H. Searls, and R. S. Windeler, "Observation of quantum-limited timing jitter in an active, harmonically mode-locked fiber laser," *Opt. Lett,* vol. 27, pp. 957, 2002.

[3] A. Schlatter, B. Rudin, S. C. Zeller, R. Paschotta, G. J. Spühler, L. Krainer, N. Haverkamp, H. R. Telle, and U. Keller, "Nearly quantum-noise-limited timing jitter from miniature Er:Yb:glass lasers," *Opt. Lett.*, vol. 30, pp. 1536-1538, 2005.

[4] S. Namiki and H. A. Haus, "Noise of the stretched pulse fiber laser. I. Theory," *IEEE J. Quantum Electron.*, vol 33, pp 649-659, May 1997.

[5] C. X. Yu, S. Namiki, and H. A. Haus, "Noise of the stretched pulse fiber laser. II. Experiments," *IEEE J. Quantum Eletron.*, vol 33, pp. 660-668, May 1997.

[6] R. Paschotta, "Noise of mode-locked lasers (Part II): timing jitter and other fluctuations," *Appl. Phys.* B, vol. 79, pp. 163-173, July 2004.

[7] F. X. Kärtner, J. Kim, J. Chen, and A. Khilo, "Photonic Analogto-Digital Conversion with Femtosecond Lasers," *Frequenz* 62, pp. 171 - 174, August 2008.

[8] Agilent Technologies, "Phase Noise Characterization of Microwave Oscillator," Product Note 11729C-2.

[9] E. N. Ivanov, S. A. Diddams, and L. Hollberg, "Study of the excess noise associated with demodulation of ultra-short infrared pulses," *IEEE Trans. Ultrason. Ferroelectr. Freq. Control*, vol. 52, no. 7, pp. 1068-1074, July 2005.

[10] T. R. Schibli *et al.*, "Attosecond active synchronization of passively mode-locked lasers by balanced cross correlation," *Opt. Lett.*, vol. 28, no. 11, pp. 947-949, June 2003.

[11] J. Kim, J. Chen, Z. Zhang, F. N. C. Wong, F. X. Kärtner, F. Loehl, and H. Schlarb, "Long-term femtosecond timing link stabilization using a single-crystal balanced cross correlator," *Opt. Lett.*, vol. 32, no. 9, pp. 1044-1046, May 2007.

[12] F. König and F. N. C. Wong, "Extended phase matching of second-harmonic generation in periodically poled KTiOPO4 with zero group-velocity mismatch," *Appl. Phys. Lett.*, vol. 84, pp. 1644 1646, March 2004.

[13] K. Safak, M. Xin, P. T. Callahan, M. Peng, and F. X. Kärtner, "All fiber-coupled, long-term stable timing distribution for free-electron lasers with few-femtosecond jitter," *Structural Dynamics*, vol. 2, issue 4, pp. 041715, June 2015.

[14] H. Li, L.-J. Chen, H. P. H. Cheng, J. E. May, S. Smith, K. Muehlig, A. Uttamadoss, J. C. Frisch, A. R. Fry, F. X. Kärtner, and P. H. Bucksbaum, "Remote two-color opticalto-optical synchronization between two passively modelocked lasers," *Opt. Lett.*, vol. 39, issue 18, pp. 5325-5328, September 2014.

[15] M. Y. Peng, P. T. Callahan, S. Valente, M. Xin, L. Grüner-Nielsen, E. Monberg, M. Yan, J. M. Fini, and F. X. Kärtner, "Long-term stable, sub-femtosecond timing distribution via a 1.2-km polarization-maintaining fiber link: approaching 10-21 link stability," *Opt. Exp.*, vol. 21, issue 17, pp. 19982-19989, August 2013.

[16] Private Communication, Cycle GmbH.

[17] J. Kim, F. X. Kärtner, and F. Ludwig, "Balanced optical-microwave phase detectors for optoelectronic phase-locked loops," *Opt. Lett.*, vol. 31, pp. 3659-3661, December 2006.

[18] J. Kim, F. Ludwig, M. Felber, and F. X. Kärtner, "Longterm stable microwave signal extraction from mode-locked lasers," *Opt. Exp.*, vol. 15, issue 14, pp. 8951-8959, July 2007.

[19] M. Y. Peng, A. Kalaydzhyan, and F. X. Kärtner, "Balanced optical-microwave phase detector for sub-femtosecond optical-RF synchronization," *Opt. Exp.*, vol. 22, issue 22, pp. 27102-27111, October 2014.

[20] M. Xin, K. Shafak, M. Y. Peng, A. Kalaydzhyan, W. Wang, O. D. Mücke, and F. X. Kärtner, "Attosecond precision multikm laser-microwave network," *Light: Science and Applications*, vol. 6, pp e16187; January 2017.

[21] P. T. Callahan, K. Safak, P. Battle, T. D. Roberts, and F. X. Kärtner, "Fiber-coupled balanced optical crosscorrelator using PPKTP waveguides," *Opt. Exp.*, vol. 22, pp. 9749-9758, April 2014.

[22] B. Jones, T. Hawthorne, P. Battle, K. Shtyrkova, M. Xin, P. T. Callahan, F. X. Kärtner, and T. Roberts, "Development of a waveguide-based optical cross-correlator for attosecond timing synchronization," *Ultrafast Optics UFO XI*, Jackson Hole, Wyoming USA, October 2017.

[23] Fujitsu Europe Press Release, "Fujitsu launches second generation ultra-fast 65 GSa/s 8-Bit ADC technology for 100G optical transport," `http://www.fujitsu.com/emea/news/pr/fseu-en_20100913-978.html` Sept. 13, 2010.

[24] Y. M. Greshishchev, J. Aguirre, M. Besson, R. Gibbins, C. Falt, P. Flemke, N. Ben-Hamida, D. Pollex, P. Schvan, and S.-C. Wang, "A 40 GS/s 6b ADC in 65 nm CMOS," *International Solid State Circuits Conference (ISSCC)*, paper 21.7, February 2010.

[25] M. Chu, P. Jacob, J.-W. Kim, M. R. LeRoy, R. P. Kraft, and J. F. McDonald, "A 40 GS/s time interleaved ADC using SiGe BiCMOS technology," *IEEE Journal of. Solid State Circuits*, vol. 45, no. 2, pp. 380-390, January 2010.

[26] R.H. Walden, "Analog-to-digital conversion in the early twenty-first century," *Wiley Encyclopedia of Computer Science and Engineering*, 1-14, September 2008.

[27] A. Khilo *et al.*, "Photonic ADC: overcoming the bottleneck of electronic jitter," *Opt. Exp.*, vol. 20, issue 4, February 2012.

[28] J. Kim, M. J. Park, M. H. Perrott, and F. X. Kärtner, "Photonic subsampling analog-to-digital conversion of microwave signals at 40-GHz with higher than 7-ENOB resolution," *Opt. Exp.*, vol. 16, issue 21, pp. 16509-16515, October 2008.

[29] Y. Han and B. Jalali, "Photonic time-stretched analog-todigital converter: Fundamental concepts and practical considerations," *J. Lightwave Tech.*, vol. 21, no. 12, pp. 3085-3103, December 2003.

[30] P. W. Juodawlkis, J. C. Twichell, G. E. Betts, J. J. Hargreaves, R. D. Younger, J. L. Wasserman, F. J. O'Donnell, K. G. Ray, and R. C. Williamson, "Optically sampled analog-to-digital converters," *IEEE Transactions on Microwave Theory and Techniques*, vol. 49, issue 10, pp. 1840-1853, October 2001.

[31] T. R. Clark, J. U. Kang, and R. D. Esman, "Performance of a time- and wavelength-interleaved photonic sampler for analog-digital conversion," *IEEE Photon. Technol. Lett.*, vol. 11, no. 9, pp. 1168-1170, September 1999.